High-cycle variable amplitude fatigue experiments and design framework for bridge welds with high-frequency mechanical impact treatment

DOI: 10.1002/stco.202200003

Poja Shams-Hakimi, Hassan Al-Karawi, Mohammad Al-Emrani

ARTICLE

High-cycle variable amplitude fatigue experiments and design framework for bridge welds with high-frequency mechanical impact treatment

Fatigue enhancement by way of high-frequency mechanical impact (HFMI) treatment can enable effective design and construction of steel bridges. However, bridges may experience high and varying mean stresses, the effects of which are not covered today by any design recommendation or in the literature on HFMI-treated joints. In this study, fatigue experiments were conducted with realistic in-service bridge loading, which revealed the same high fatigue performance as for constant amplitude loading. The effect of mean stress in spectrum loading was quantified and a method to account for it in an equivalent manner is proposed. A design framework has been developed for design and engineering purposes.

Keywords fatigue enhancement; bridge; variable amplitude; mean stress; design

1 Introduction

In the design of steel bridges, fatigue failure at the weld toe often governs the design and therefore plays a crucial role in the choice of steel grade and amount of steel used. The fatigue performance of conventional welds is independent of steel grade, and very little can be done in the execution or design of the welds to improve the fatigue strength significantly. The fatigue design requirements are therefore usually met by increasing the plate thicknesses to reduce the stresses, and the steel grades commonly used remain limited to S355, S420 and S460 [1].

Employing high-frequency mechanical impact (HFMI) treatment to enhance the fatigue strength means it is possible to use higher-strength steels and thinner plates in bridges. High-strength steels and thin plates contribute to an additional increase in fatigue performance [2, 3] and can significantly reduce the welding work. Therefore, HFMI treatment implies great potential for reducing material consumption and making the design and construction of bridges more effective [4].

HFMI treatment induces compressive residual stresses at the locations of crack initiation and significantly delays the formation of cracks, resulting in a considerable increase in fatigue strength. However, owing to the high reliance on the induced residual stresses, the fatigue performance of HFMI-treated welds is also very dependent on the loading characteristics. Load situations that may impair the fatigue performance of HFMI-treated joints include high mean tensile stresses [5–7] and large load cycles that cause excessive local yielding at the weld toe [6, 8–10]. Load cycles with high mean tensile stresses temporarily reduce the beneficial compressive residual stresses from HFMI treatment, causing the succeeding load cycles to become more damaging. Excessive local yielding, on the other hand, can partially or fully relax the induced stresses and reduce the fatigue strength permanently. Furthermore, for variable amplitude (VA) loading with a fluctuating mean stress, previous studies have found the fatigue strength to be lower than in cases with a constant mean stress [11]. This additional damaging effect is not captured by regular mean stress correction methods; instead, studies have proposed a low damage sum of 0.2 at the failure to account indirectly for this phenomenon [12]. However, the International Institute of Welding (IIW) recommends using an allowable damage sum of 0.5 [13].

Many experimental VA studies of HFMI specimens have been reported in the literature and a review of these studies by the authors can be found in [14]. Conversely, only a few studies have investigated HFMI specimens subjected to bridge loading [15–17]. However, these studies did not include the mean stresses that are common in real bridges. In their investigations of non-loadbearing transverse attachment joints under bridge loading, Ghahremani et al. [17] showed that the HFMI performance was as good at a low mean stress VA loading as for the case of a constant amplitude (CA) $R = 0.1$ loading. Furthermore, they showed that variations in mean stress in the VA loading cycles were insignificant for fatigue performance. Tai and Miki [16], on the other hand, found that the performance of longitudinal attachment specimens subjected to bridge VA loading was significantly poorer compared with the CA $R \approx 0$ loading, although still representing a major improvement compared with the as-welded state [16]. The review in [14] shows that the observed decrease in HFMI fatigue performance for VA loading appears to be related to the type of specimen investigated. It was clear that longitudinal attachment specimens performed much less well under VA compared with CA loading, whereas transverse attachment specimens performed equally well. Nevertheless, the test results in all studies were conservatively predicted by the fatigue curves provided by the IIW for the $R = 0.1$ loading. This was partly possible because the VA studies in the literature almost exclusively included low overall mean stresses. No systematic investigations of the

mean stress effect nor high mean stress experiments were found in the literature.

In the previous publication by the authors [14], an assessment of realistic in-service stresses in four case-study composite steel and concrete road bridge was made assuming HFMI treatment of the critical welds. It was shown that the in-service stresses can reach very high overall mean values due to high stresses from permanent loads, including the self-weight stresses of steel, concrete and pavement. Furthermore, in fatigue-critical locations, both the mean stresses and the stress ratios were shown to vary due to the variations in the traffic load. The two properties of high and variable mean stresses together make it difficult to consider the mean stress effect in bridge design. This is because, on the resistance side, no single *SN* curve can be used that is suitable in terms of a mean stress, whereas, on the load side, the Palmgren-Miner's equivalent stress range does not account for the damaging effect of the mean stresses. These challenges exist even though the stress range spectrum and its relationship to the variations in mean stress are known. In cases where they are not known, such as in bridge design situations, empirical methods based on specific traffic data must be developed to account for the mean stress effect.

The main aims of this study are to study experimentally the performance of HFMI-treated specimens subjected to VA bridge loads and to develop a design framework that accounts for varying mean stresses in the fatigue design of HFMI-treated joints. This was achieved through cycle-by-cycle random sequence fatigue testing with an empirically derived road bridge spectrum, together with mean stresses relevant to composite steel and concrete bridges. Low mean stress VA experiments were also conducted to investigate whether the VA load is detrimental to fatigue performance. Thereafter, the effect of mean stress under spectrum loading was quantified experimentally and an approach to include it in a modified equivalent stress range was proposed. The design framework was then developed and verified against both the VA experiments and the case-study bridges in [14]. This framework agrees with the most common fatigue verification method in the Eurocodes [18]: the damage equivalent factor method, also referred to as the lambda method. Some of the conclusions from the experiments were that typical bridge VA loads with a low mean stress have no detrimental effect on the fatigue performance of transverse attachment joints, compared with the CA R = 0.1 strength. On the other hand, the experimental results clearly show that high minimum stresses, corresponding to stresses due to permanent loads in bridges, significantly reduce the endurable number of load cycles [14]. Furthermore, based on only one experiment, it was observed that large compressive preloads dramatically reduce the fatigue strength and must therefore be avoided after HFMI treatment.

In bridge design with HFMI treatment, there are two alternative scenarios that consider the influence of self-weight stresses on the mean stress effect: The first scenario involves HFMI treatment after the erection of a bridge, where the induced compressive stresses from HFMI treatment are expected to be unaffected by the self-weight. In this scenario, the local mean stresses at the weld toe will be low, resulting in a high fatigue improvement effect [8, 19–21]. The second scenario is where HFMI treatment is performed in the fabrication shop, before bridge erection. In the event of tensile self-weight stresses, the compressive stresses from the treatment will be reduced and this will result in a higher local mean stress, which reduces the fatigue strength. This paper focuses on the latter alternative.

2 Fatigue test programme

2.1 Test specimens

In this study, 14 VA high-cycle fatigue tests were performed on non-loadbearing transverse attachment specimens. Two of the tests were conducted on specimens in the as-welded (AW) state. Four were HFMI low mean (LM) stress tests and eight were HFMI high mean (HM) stress tests. One of the HFMI-HM specimens was tested with five compressive preloads prior to fatigue loading. Fig. 1 shows the test setup and specimen dimensions.

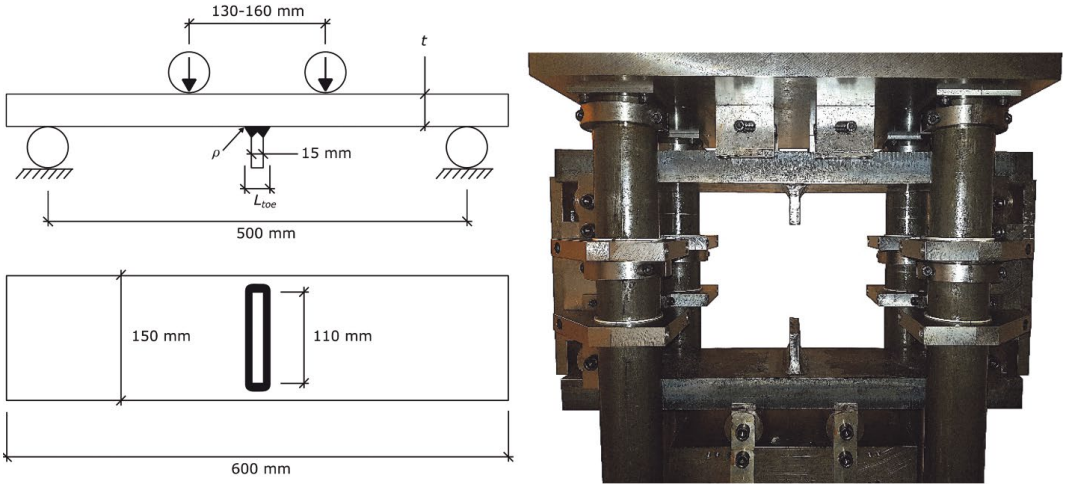

Fig. 1 Test specimen dimensions and loading arrangement

Tab. 1 Specimen overview and mechanical properties according to manufacturer

Series	t [mm]	Steel grade	f_y [MPa]	f_u [MPa]	Elongation [%]	k
AW	38	S460M	562	659	22	2
HFMI	40	S460M	566 (524*)	639	23	12

*Based on additional tensile tests performed at Chalmers

k = number of fatigue-tested specimens

The average weld toe radius of the HFMI specimens was ρ = 2.7 mm and the average toe-to-toe distance was L_{toe} = 30 mm, established through laser scanning. The HFMI specimens in this study were made with t = 40 mm base plate thickness, whereas t = 38 mm was used for the AW specimens.

The fatigue testing was performed at Chalmers University of Technology with a machine that was capable of testing two specimens simultaneously. The CA R = 0.1 fatigue strengths at two million cycles were previously established for 280 MPa with an *SN* slope of m = 6.5 and for 150 MPa with m = 3.1 for the HFMI and AW specimens respectively [22]. The CA and VA specimens were all manufactured at the same time by the same welder and HFMI operator. More details on the manufacturing can be found in [22], along with chemical composition, residual stress measurements, weld toe scanning results and microstructure investigations. Tab. 1 summarizes the properties of the specimens used in this study. Owing to the great difference between the nominal yield stress (460 MPa) and the yield stress specified by the steel manufacturer (566 MPa), additional static tensile tests were conducted to verify the yield stress. An average yield stress of 524 MPa was obtained from the tensile tests.

2.2 Fatigue loading

The fatigue testing was performed at room temperature with load frequencies of 10–20 Hz depending on the load level. The loading was carried out with force control according to a cycle-by-cycle random sequence load history. Testing was terminated at half-thickness cracks, triggered by displacement criteria for the load actuator which corresponded to a certain drop in stiffness in the specimens. When the crack reaches half-thickness, negligible fatigue life remains to cause a complete fracture, as shown in crack propagation curves in [15].

The VA load that was chosen for the experiments described here was based on a bridge stress assessment study performed by the authors in [14] which included four existing case-study bridges with different spans and numbers of spans (1, 2, 3 and 5). The simply supported bridge, which had a span of 32 m, was shown to experience the most severe spectrum shape and the most unfavourable mean stresses. The load history of this bridge was therefore chosen for this experimental investigation.

Rainflow analysis in accordance with [23] was performed on the VA load history to produce stress range spectra. Fig. 2 shows the normalized stress range spectrum with two different forms: a) histogram and b) cumulative frequency distribution. The original spectrum had a sequence length of 55 000 cycles but was truncated in order to reduce testing time. Based on the CA curve of the AW test specimens, the lower portion of the spectrum that represented 5 % of the total damage was determined and used as the omission strategy for small stress ranges, resulting in a reduced sequence length of 34 466 cycles. This omission represented a damage percentage substantially smaller than 5 % for the HFMI specimens, as the *SN* slope was shallower in that case. The sequence order was randomized once but was kept the same for all specimens,

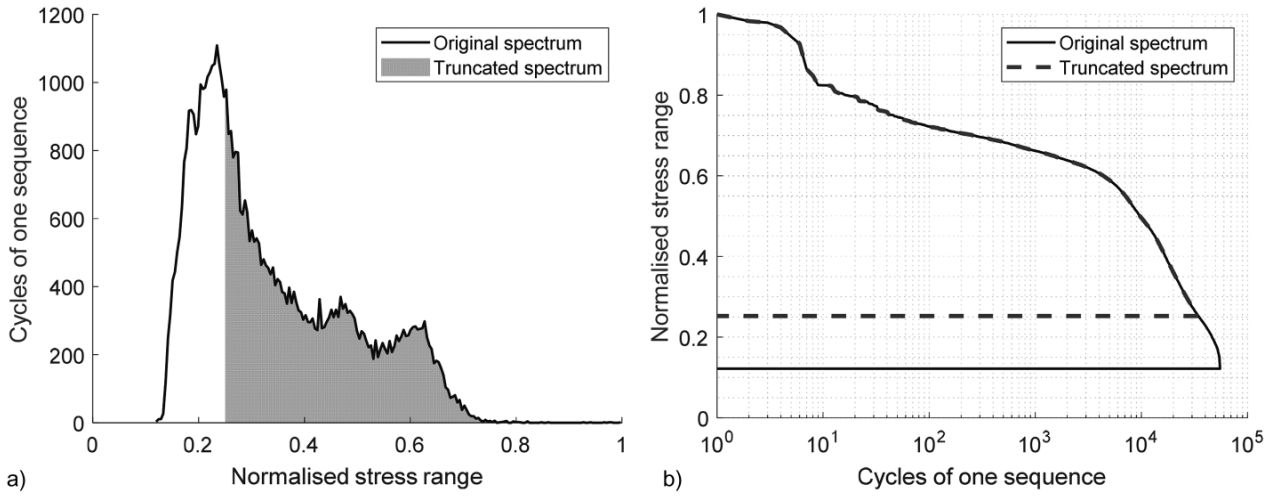

Fig. 2 The normalized stress range spectrum in the form of a) histogram, and b) cumulative frequency distribution

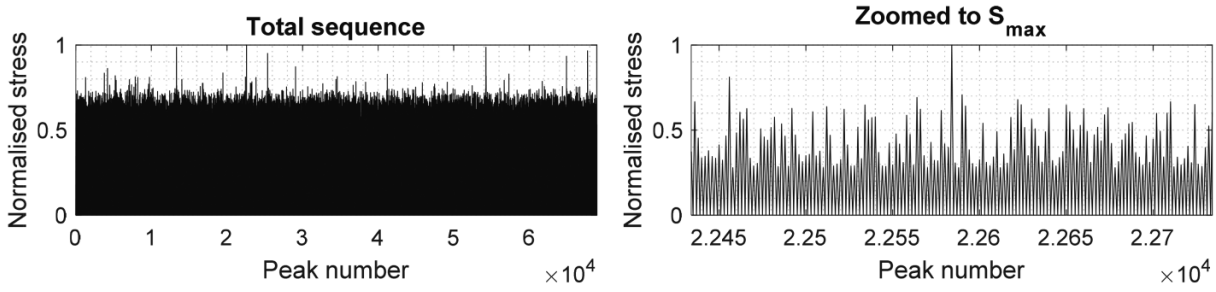

Fig. 3 Normalized random sequence with minimum stresses equal to zero (highest stress peak in sequence enlarged in right-hand diagram)

see Fig. 3. As a property of the simply supported bridge at mid-span, the minimum stresses of all load cycles were constant and representative of the self-weight stress.

The HFMI specimens were divided into two main groups: low mean (LM) and high mean (HM). In the LM group. The maximum stress in the sequence was kept at about $0.8f_y$, while the minimum stresses were kept at approx. 20 MPa, resulting in low overall stress ratios. In the HM group, on the other hand, two levels of higher minimum stress were used to represent the self-weight stress of composite steel and concrete bridges, while the maximum stress was still kept at approx. $0.8f_y$ (subgroups HM1 and HM2). For one high-mean specimen (HM3), a somewhat lower maximum stress was chosen in order to achieve stress ranges similar to those expected in bridges [14]. Lastly, one specimen (HM4) was subjected to stresses similar to those for HM3, but, prior to fatigue loading, five compressive preloads of approx. $-0.9f_y$ (–480 MPa) were applied to simulate unfavourable conditions during the construction phase. The AW specimens were both subjected to load conditions comparable to HM3, i.e. high minimum stresses and realistic equivalent stress range magnitudes. However, one of the AW specimens was subjected to the full spectrum without stress range omission in order to verify the assumption regarding the damaging effect of small stress ranges.

2.3 Fatigue test results

All the stress results in this section are derived from the output data of the testing machine. They were calculated by converting the output forces into stresses, considering roller distances, main plate thickness and main plate width, all of which were measured for every test. The conversion from applied force to nominal stress was verified with strain gauge measurements. Tab. 2 summarizes the results, including the basic nominal stresses, stress ratios and the number of cycles to failure. All failures occurred at the weld toe, see Fig. 4 for an example.

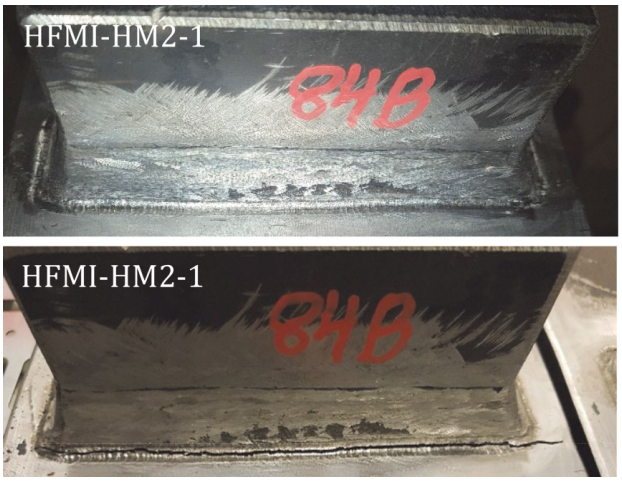

Fig. 4 Example of an HFMI-treated weld before and after failure

Tab. 2 Basic VA fatigue experiment results

Specimen	S_{max}	S_{min}	ΔS_{max}	ΔS_{min}	R_{max}	R_{min}	R_{avg}	N_f	Description
AW-1	386	190	196	38	0.83	0.49	0.71	11 547 516	Truncated spectrum
AW-2	366	189	177	5	0.97	0.52	0.80	19 865 882	Full spectrum
HFMI-LM-1	435	17	418	106	0.14	0.04	0.10	10 732 297	Low mean
HFMI-LM-2	435	20	415	104	0.16	0.05	0.09	12 330 575	Low mean
HFMI-LM-3	419	23	396	98	0.19	0.05	0.12	21 393 484	Low mean
HFMI-LM-4	427	21	407	103	0.17	0.05	0.11	30 892 827	Low mean
HFMI-HM1-1	426	126	300	68	0.65	0.30	0.52	11 244 773	High mean level 1
HFMI-HM1-2	429	126	303	69	0.65	0.29	0.52	13 052 850	High mean level 1
HFMI-HM2-1	427	194	234	55	0.78	0.45	0.67	5 796 948	High mean level 2
HFMI-HM2-2	424	192	232	56	0.77	0.45	0.67	13 096 410	High mean level 2
HFMI-HM2-3	424	193	231	56	0.78	0.46	0.67	29 530 032	High mean level 2
HFMI-HM2-4	428	191	237	59	0.76	0.45	0.66	53 752 303	High mean level 2
HFMI-HM3-1	388	188	200	51	0.79	0.48	0.68	89 302 861	High mean with realistic stress ranges
HFMI-HM4-1	375	195	179	41	0.83	0.52	0.74	8 092 180	Five preloads of –480 MPa, thereafter high mean with realistic stress ranges

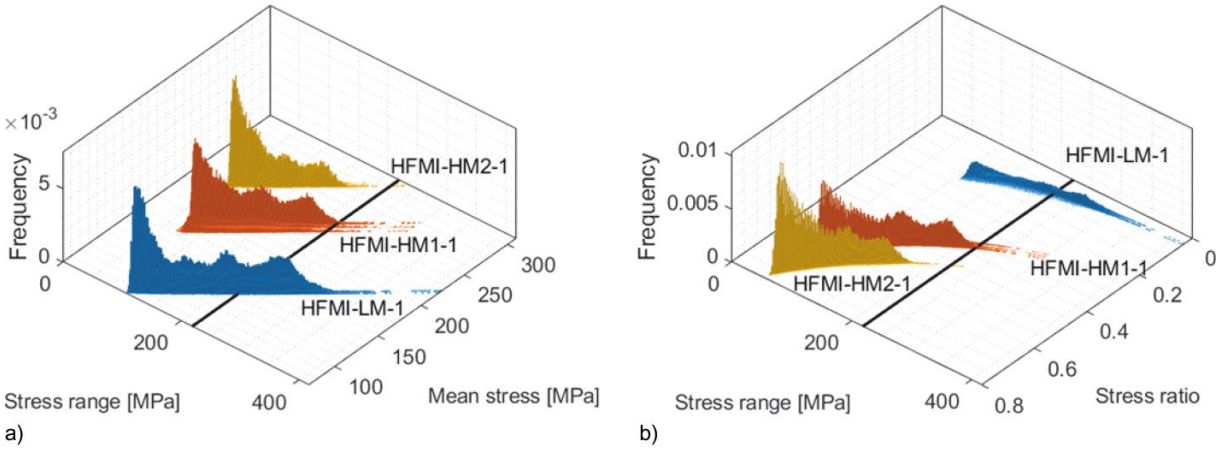

Fig. 5 Rainflow matrices for three example specimens showing a) mean stresses, and b) stress ratios (stress range corresponding to 10 million cycles for CA HFMI fatigue strength also indicated)

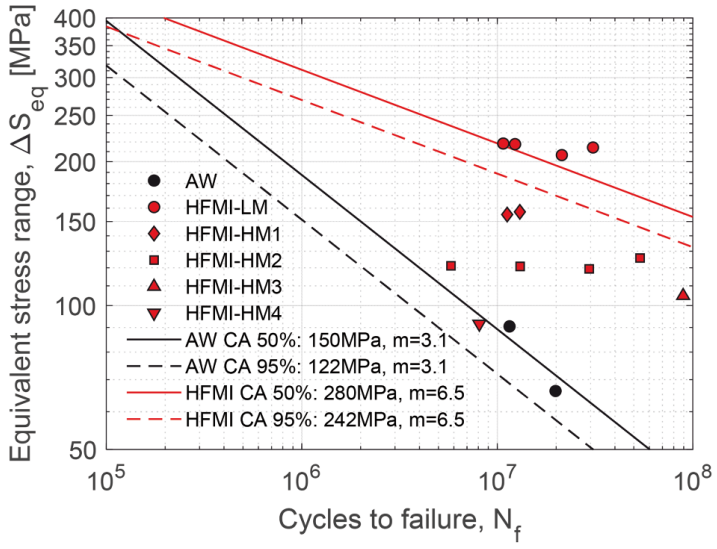

Specimen	ΔS_{eq}	Nf
AW-1	90,5	11 547 516
AW-2	66,3	19 865 882
HFMI-LM-1	218,4	10 732 297
HFMI-LM-2	217,7	12 330 575
HFMI-LM-3	206,6	21 393 484
HFMI-LM-4	214,3	30 892 827
HFMI-HM1-1	155,1	11 244 773
HFMI-HM1-2	157,1	13 052 850
HFMI-HM2-1	121,2	5 796 948
HFMI-HM2-2	120,8	13 096 410
HFMI-HM2-3	119,4	29 530 032
HFMI-HM2-4	125,8	53 752 303
HFMI-HM3-1	104,9	89 302 861
HFMI-HM4-1	91,6	8 092 180

Fig. 6 Equivalent stress ranges with single-slope Palmgren-Miner's sum according to Eq. (1) compared with experimental CA $R = 0.1$ curves from [22]

Three specimens that were representative of their groups were used to produce Rainflow matrices, including both mean stress and stress ratio, see Fig. 5. The HFMI-LM specimen contained the largest stress ranges and its histogram shape was more "stretched out" compared with the HM specimens, due to the large scaling of the ranges. Moreover, Fig. 5 shows that low stress ranges were associated with high stress ratios and that the variation in stress ratio within the same loading increased with the increase in overall mean stresses. The stress range that corresponded to 10 million cycles on the experimental CA curve for HFMI is also shown in Fig. 5 to indicate the proportions of the spectra above or below that level. The 10 million cycles limit represents the knee point of the bilinear *SN* curves given by the IIW and its influence on the results will be presented later in this paper.

First, the single-slope equivalent stress range based on Palmgren-Miner's damage sum according to Eq. (1) was used in order to compare the VA test results with the mean experimental CA $R = 0.1$ fatigue curves from [22], see Fig. 6. In Eq. (1), ΔS_i is the stress range of the ith load cycle in the spectrum and n_i is the number of occurrences associated with that cycle. The slopes of the *SN* curves obtained from the CA fatigue tests [22] were used to calculate the equivalent stress ranges. This equivalent stress range does not include the effect of mean stress. The following can be observed in Fig. 6: The AW specimens both correspond well with the mean AW CA curve despite the high and non-constant mean stresses and the fact that one specimen was tested with the full spectrum and one with the truncated spectrum. Similarly, the HFMI-LM specimens all performed equally well or better than the mean HFMI CA strength. This indicates that the low mean stress VA loading, including the variations in mean stress, did not influence the fatigue performance negatively and could be properly represented with Eq. (1) for the HFMI-treated joints. The results of the HM1, HM2 and HM3 specimens clearly show the detrimental effect of the high mean stresses and are therefore not comparable with the CA $R = 0.1$ strength. Unfortunately, a wide scatter was seen for the HM2 group. The reason for this is not clear to the authors, but the matter is further elaborated on in the discussion below. The HM4 specimen, which was subjected to five compressive preloads prior to fatigue loading, performed much more poorly than the

HM3 specimen, for example. However, HM4 being situated down on the AW curve, was due not only to the preloads but also the high mean stresses.

$$\Delta S_{eq} = \sqrt[m]{\frac{\Sigma\left(n_i \cdot \Delta S_i^{\,m}\right)}{\Sigma n_i}} \quad (1)$$

3 Considering the mean stress effect

In the IIW recommendations [24], the detrimental effect of a high mean stress is accounted for by reducing the fatigue strength (FAT) of HFMI-treated joints for different intervals of stress ratio. This stepwise method is well established and is suitable for CA applications. Owing to its discrete nature, however, the IIW method is less suitable for VA applications with varying stress ratios. Furthermore, the method is currently only applicable for stress ratios up to $R = 0.52$. Mikkola et al. [25] proposed an extension of the method to $R = 0.7$ and, since then, 36 more *SN* data points with stress ratios of $0.5 < R \leq 0.8$ have been published [26, 27]. Upon preliminary examination, these data appear to support the trends in the IIW model for higher R values as well.

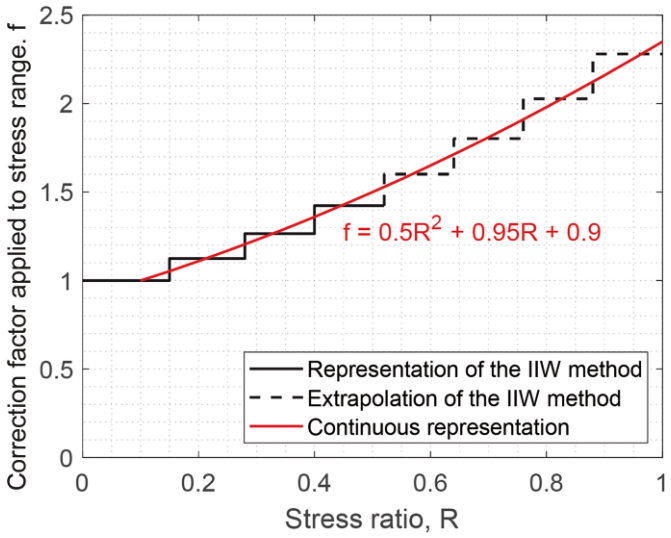

Fig. 7 Illustration of proposed continuous mean stress correction implemented here and underlying stepwise method

The IIW stress ratio correction has been adopted here, but with some suggested modifications to make it suitable for VA applications. Firstly, instead of reducing the *fatigue strength* for high stress ratio cycles ($R > 0.1$), the *stress ranges* of these cycles were magnified, keeping the fatigue strength unchanged as the CA $R = 0.1$ strength. For instance, if the fatigue strength were to be reduced by one FAT class according to the IIW, a factor of 1.125 would instead be applied to the stress range, which is approximately equivalent. Moreover, the IIW method was extrapolated to $R = 1.0$ and a polynomial fit was used to represent the method in a continuous manner, see Fig. 7. In principle, the trend follows an increase of 12.5 % in correction factor per 0.12 increase in R. The continuous approach for mean stress correction is suitable for VA applications, especially as it allows the equivalent stress range to be modified to include the stress ratio effect, as proposed in Eq. (2). The magnification factor f_i is the correction factor according to the polynomial in Fig. 7 for the stress ratio of each cycle R_i, see Eq. (3). No f_i values < 1.0 were allowed and, in cases of stress cycles with $R_i < 0.1$, f_i was set to 1.0.

$$\Delta S_{eqR} = \sqrt[m]{\frac{\Sigma\left(n_i \cdot (\Delta S_i \cdot f_i)^m\right)}{\Sigma n_i}} \quad (2)$$

$$f_i = 0.5R_i^2 + 0.95R_i + 0.9 \quad (3)$$

Correcting the stress ranges according to Eq. (2) means that the modified equivalent stress ranges obtained ΔS_{eqR} represent the $R = 0.1$ loading and can therefore be compared with the CA curves. Again, the natural slope of the CA *SN* curve ($m = 6.5$) was used to calculate ΔS_{eqR}. It can be seen from Fig. 8 that almost all the HFMI VA results lie above the mean CA strength and only one of the HM2 points was below the characteristic strength. Of course,

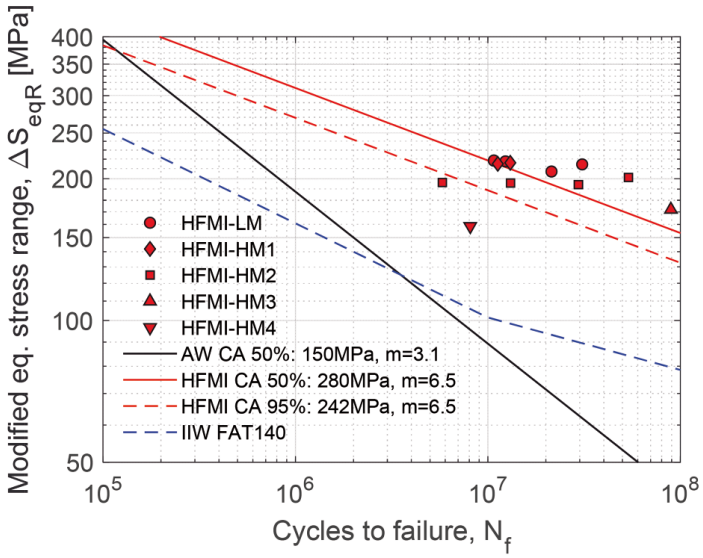

Specimen	Δ S eqR	N f
HFMI-LM-1	218,5	10 732 297
HFMI-LM-2	217,7	12 330 575
HFMI-LM-3	207,1	21 393 484
HFMI-LM-4	214,5	30 892 827
HFMI-HM1-1	215,1	11 244 773
HFMI-HM1-2	216,2	13 052 850
HFMI-HM2-1	196,3	5 796 948
HFMI-HM2-2	195,8	13 096 410
HFMI-HM2-3	194,3	29 530 032
HFMI-HM2-4	201,2	53 752 303
HFMI-HM3-1	172,0	89 302 861
HFMI-HM4-1	158,5	8 092 180

Fig. 8 Equivalent stress ranges according to Eq. (2), modified to include the mean stress effect, compared with experimental CA $R = 0.1$ curves from [22]

Tab. 3 Severity of mean stress effect and real damage sums

Specimen	$\Delta S_{eqR} / \Delta S_{eq}$	D_{real}
HFMI-LM-1	1.0	1.1
HFMI-LM-2	1.0	1.2
HFMI-LM-3	1.0	1.5
HFMI-LM-4	1.0	2.7
HFMI-HM1-1	1.4	1.0
HFMI-HM1-2	1.4	1.2
HFMI-HM2-1	1.6	0.3
HFMI-HM2-2	1.6	0.6
HFMI-HM2-3	1.6	1.4
HFMI-HM2-4	1.6	3.1
HFMI-HM3-1	1.6	1.9
HFMI-HM4-1	1.7	0.1

the preloaded specimen (HM4-1) was significantly below the HFMI CA strength, but clearly still lies well above the mean AW CA curve. Moreover, it can be seen that HM1 specimens are situated very close to LM specimens, whereas, for higher cycles to failure ($> 10^7$), the trends seemingly indicate a shallower slope. This subject is further investigated below. Overall, the results indicate that the bridge VA load in itself does not reduce the fatigue strength, but high overall mean stresses and large compressive preloads do. Evidently, all the data points were situated significantly above the FAT 140 strength recommended by the IIW for the $R = 0.1$ loading on this specimen type and the current yield stress [24].

The real damage sums are given in Tab. 3. They were taken as the actual number of cycles to failure divided by the predicted number of cycles, using ΔS_{eqR} with the CA curve established in a previous study [22] for these specimen types. This is in accordance with the IIW recommendations. Excluding the preloaded specimen (HM4-1), the average real damage sum was 1.4.

Tab. 3 also includes the severity of the mean stress effect, represented for all specimens by the ratio of the modified equivalent stress range to the regular stress range. For the experiments, this ratio represents the combined detrimental effects of the minimum stress and the stress ratio content in the load, because the maximum stresses were fairly similar in all experiments. For a bridge design situation, this ratio corresponds to the combined effects of the self-weight proportion of the total load and the stress ratio content due to the traffic composition. A method able to distinguish these two effects and provide this ratio for any self-weight and traffic load proportion would be very useful in design situations. To this end, the next section presents a proposal for a method of this kind.

4 Proposed design framework

The previous section showed that ΔS_{eqR} in combination with the suggested continuous mean stress correction was able to represent the VA load, including the mean stresses, in an equivalent manner and enable the comparison with the CA fatigue strength. As a result, the $\Delta S_{eqR}/\Delta S_{eq}$ ratio is a representative parameter that describes the severity of the mean stress effect in the spectrum. This parameter is hereinafter referred to as λ_{HFMI}, see Eq. (4).

$$\lambda_{HFMI} = \frac{\Delta S_{eqR}}{\Delta S_{eq}} \tag{4}$$

If λ_{HFMI} can be predicted in a simple manner, then any ΔS_{eq} based on the same or a similar spectrum as the λ_{HFMI} could be enlarged to obtain ΔS_{eqR}. However, as mentioned in the introduction and evident from the experiments, detailed knowledge of the VA load – seldom available to the designer – is necessary in order to calculate an exact λ_{HFMI} value. The work of generalizing λ_{HFMI} for road bridges is presented below and a design framework is proposed so that the engineer can obtain a reasonable approximation of λ_{HFMI}. The framework is adapted to agree with the currently most common and simplest fatigue verification method in the Eurocodes, the lambda method (damage equivalent factor method). The same concept can be implemented in future research to generalize λ_{HFMI} for other applications as well, e.g. for railway bridges.

For road bridges, the lambda method involves calculating a stress range ΔS_p generated by a load model FLM 3 and converting this stress range into an equivalent stress range representative of the fatigue damage due to real traffic [18]. This is done simply by using a set of λ factors that are multiplied by ΔS_p. Here, it is postulated that an additional λ factor, the λ_{HFMI}, can be used to account for the mean stress effect by enlarging the conventional equivalent stress range obtained by the lambda method. Of course, both λ_{HFMI} and the original λ factors must represent different characteristics of the real traffic sufficiently well.

The new factor λ_{HFMI} needs to account for the stress ratio content of the real traffic (1), the stress ratio contribution from the self-weight (2) and the relationship of fatigue strength to mean stress or stress ratio (3). Point (1) was achieved by producing influence lines for different locations on bridges with various spans ($10 \le L \le 80$ m) and running the same measured traffic loads used for the fatigue experiments over these influence lines. Five different locations were studied on continuous symmetrical double-span bridges with constant bending stiffness (prismatic beams); mid-span $0.50L$, intermediate locations $0.75L$, $0.85L$ and $0.95L$, and mid-support $1.0L$. In addition, the mid-span of simply supported bridges was included. After considering several different alternatives to represent the influence of self-weight, point (2), a ratio Φ of the self-weight stress to the maximum stress range coming due to traffic $\Phi = S_{SW}/\Delta S_{max}$ was considered the most appropriate. This effect was included in the investigation by normalizing the traffic load with respect to the maximum stress range and presuming an interval of Φ values from 0 to 9. Lastly, mean stress correction factors according to Eq. (3) were incorporated. Both the Palmgren-

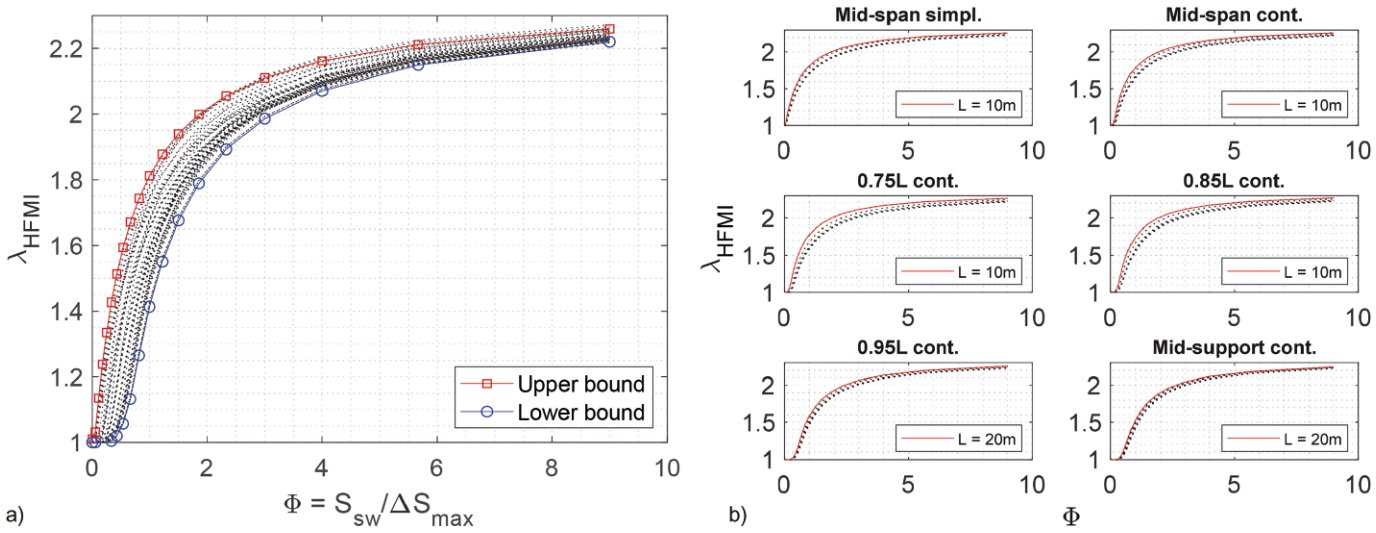

Fig. 9 a) All generated Φ-λ_{HFMI} curves, and b) Φ-λ_{HFMI} curves categorized by bridge location (red lines = spans generating upper bound Φ-λ_{HFMI} curve at each bridge location)

Miner's equivalent stress range ΔS_{eq} and the modified range according to Eq. (2) ΔS_{eqR} were calculated for all cases with an *SN* slope $m = 5$, as has been established for HFMI-treated joints [24]. Finally, Φ-λ_{HFMI} curves could be produced; they are shown in Fig. 9a. The upper bound case consisted of the mid-span location of the simply supported bridge with $L = 10$ m, whereas the lower bound was found at the mid-support location of the continuous bridge with $L = 40$ m.

Apparently, the Φ-λ_{HFMI} relationship could not be generalized to just one case, since the difference in the upper and lower bounds was considerable, particularly for small Φ values. Closer inspection of the curves generated revealed that, for each bridge location, a certain span was "governing", i.e. producing, the highest Φ-λ_{HFMI} curve. However, that variation in span had a fairly small effect on the results, see Fig. 9b. For instance, for the mid-span locations, the highest Φ-λ_{HFMI} curve was for $L = 10$ m. Longer spans of up to 30 m reduced the curves somewhat, whereas for longer spans, the curves remained unchanged compared with $L = 30$ m. The reason for this observation is that, for small spans (short influence lines) relative to vehicle lengths, the stress cycles generated become more sensitive to the truck bogie or axle configurations. As a result, additional smaller cycles can occur, see Fig. 10, which compares the stress variation over time at mid-span of a simply supported bridge due to a single-bogie versus a double-bogie load.

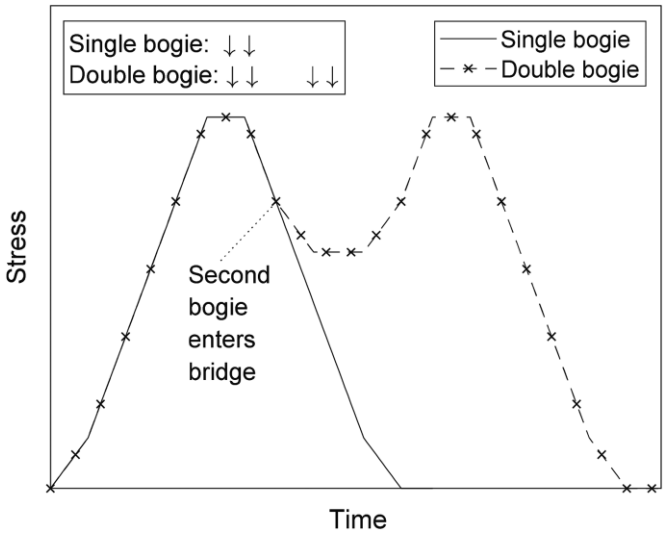

Fig. 10 Simplified example of the effect of short influence lines on the generation of additional small cycles with higher mean stresses

The influence line is long compared with the single-bogie load and, as a result, only one stress cycle occurs. On the other hand, the influence line is relatively short compared with the double-bogie load. By the time the second bogie enters the bridge, the first has just passed mid-span. From this point in time until the second bogie reaches mid-span, an additional smaller stress cycle is produced. The minimum stresses of these additional cycles are usually higher compared with those of the main cycles and therefore contribute to a higher mean stress effect. As a result, a higher λ_{HFMI} value is obtained for these cases. Similar observations were made for all the bridge locations investigated for small spans.

To simplify the approach, only the span with the highest λ_{HFMI} values was chosen to represent each location, i.e. the continuous red lines in Fig. 9b. Fig. 11a compares the different locations with an enlarged Φ scale. The highest λ_{HFMI} values are found at mid-span of the simply supported case, followed by mid-span for the continuous case. For the rest of the locations, the Φ-λ_{HFMI} curves gradually decreased as the location approached mid-support. This observation reflects the shapes of the influence lines, which also gradually decrease in mean value as the location approaches mid-support, see Fig. 11b.

In order to produce a conservative design and follow the same definition of span and support regions as given in the Eurocode [18] (Fig. 12b), the Φ-λ_{HFMI} curve for the simply supported case is proposed for all mid-span sec-

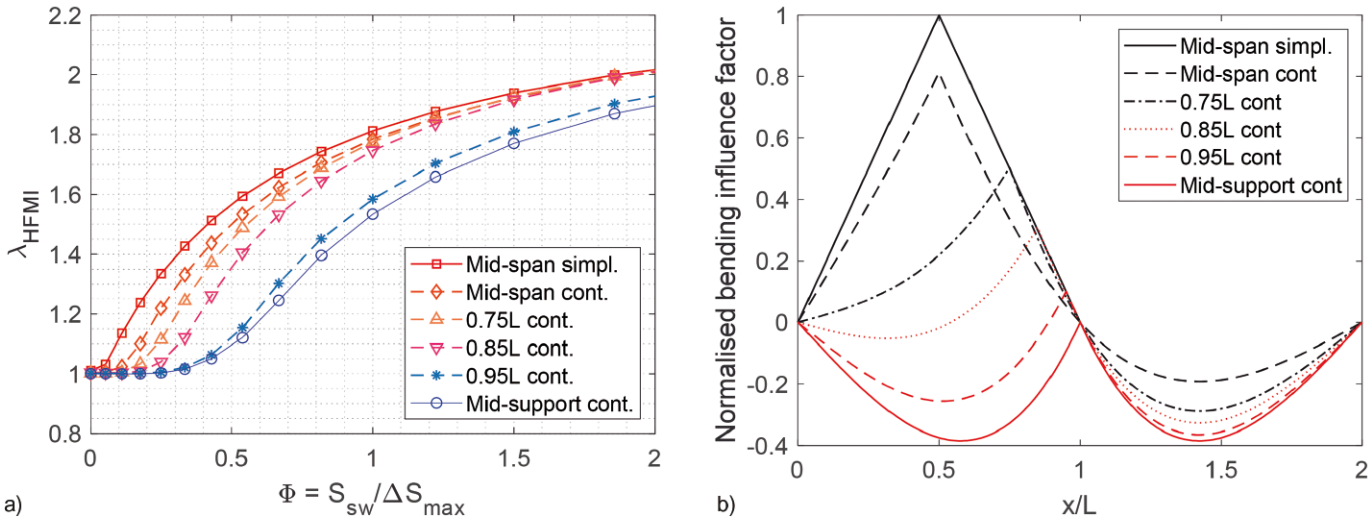

Fig. 11 a) Comparison of Φ-λ_{HFMI} curves for different bridge locations, and b) decreasing mean value of influence lines as the location approaches mid-support

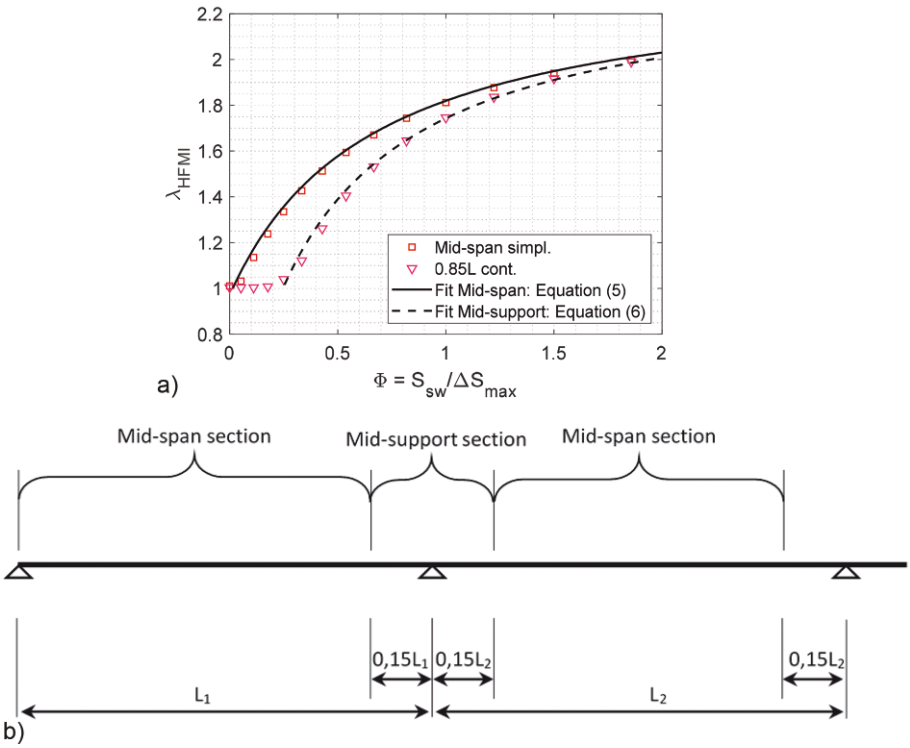

Fig. 12 a) Φ-λ_{HFMI} curves proposed for the design of mid-span and mid-support sections, and b) definition of regions where these sections apply, adapted from [18]

tions, including end-support regions. The curve for the 0.85L location is proposed for all mid-support sections. Fig. 12a shows the proposed curves for design purposes which were fitted to the data with expressions according to Eqs. (5) and (6). If the fitted expressions generate $\lambda_{HFMI} < 1.0$, then that value should be replaced by 1.0.

$$\text{Mid-span:} \quad \lambda_{HFMI} = \frac{2.38\Phi + 0.64}{\Phi + 0.66} \tag{5}$$

$$\text{Mid-support:} \quad \lambda_{HFMI} = \frac{2.38\Phi + 0.06}{\Phi + 0.40} \tag{6}$$

In order to calculate Φ, the maximum stress range due to traffic is required ΔS_{max}. As the last stage of framework development, a practical method for obtaining ΔS_{max} is proposed by finding its relationship to the stress range from FLM3 (ΔS_p), which is a parameter known to the designer. For this purpose, the ratio of the traffic-induced maximum stress range to the stress range generated from FLM3 is illustrated in Fig. 13. Although clear dependence on span can be seen in Fig. 13, with some difference between the bridge locations, it is suggested that $\Delta S_{max}/\Delta S_p$ be set at a constant value of 2.0 for all cases. This simplification reduces the complexity of the approach dramatically at the expense of a minor loss in accuracy. The effect of this simplification on the final λ_{HFMI} values is a conservative prediction of up to 3 % for ratios > 2.0 and a liberal prediction of up to 2 % for ratios < 2.0. The ratio of the traffic-induced maximum stress ranges to that generated by any other reference load can be derived in a similar way.

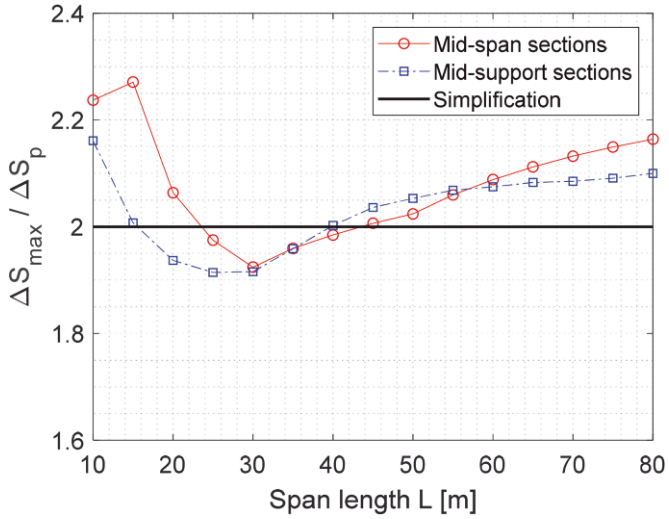

Fig. 13 Ratio of traffic-induced maximum stress range ΔS_{max} to stress range from fatigue load model 3 ΔS_p

5 Discussion

5.1 The VA experiments

As is shown in Fig. 8, the high-mean VA data are significantly elevated when the mean stress effect is included in the equivalent stress ranges. The first question that arises is how sensitive is this elevation with respect to the assumed extrapolation of the IIW mean stress correction, i.e. for $R > 0.52$. To investigate this, the fatigue test data were re-evaluated, assuming that the correction factors were constant and equal to $f = 1.53$ for $R_i > 0.52$. Of course, this was only done as a means of sensitivity analysis. The investigation showed that, like the LM group, the HM1 group remained unchanged after modifying the mean correction curve, since the stress ratios of the largest stress cycles were predominantly below $R = 0.52$ (see Fig. 5b). On the other hand, the HM2 and HM3 groups, which had most of their stress ratios above $R = 0.52$, were elevated to a lesser extent than before, resulting in lower real damage sums. Nevertheless, only one additional point fell below the CA curve, the HM2-3 specimen, for which the real damage sum changed from 1.4 to 0.9. The average of all damage sums was still 1.25. This sensitivity check strengthens the notion that the modified equivalent stress range, Eq. (2), together with the mean stress correction, Eq. (3), represent HFMI VA data appropriately.

The second question is whether the VA fatigue test results would be better represented by a double-sloped *SN* curve compared with the single slope of $m = 6.5$. To investigate this, a knee point was presumed at 10 million cycles, as suggested by the IIW [24]. The CA curve with a fatigue strength of 280 MPa and slope $m = 6.5$ was used before the knee point, whereas the slope after the knee point could vary between 6.5 and 22, with 0.5 increments. All HFMI data points except HM4-1 were included and the modified equivalent stress ranges were re-evaluated for each slope increment, while the sum of the squared errors was registered. The double-slope expression given by the IIW [24] was used to calculate the equivalent stress ranges, but with the modification that each stress range was multiplied by f_i from Eq. (3). The result is shown in Fig. 14. The best fit was achieved for the second slope of 14.5 with significantly less scatter compared with the single-slope case and a sum of the squared errors equal to 2×10^{15}. The corresponding value for the single-slope case was 4×10^{15}. The results appear to confirm the frequently used formulation for the second slope according to Haibach [28]: $m_2 = 2m_1 - 1$. Using this formulation results in the second slope of $m_2 = 12$, which, according to Fig. 14, would still give a small value for the sum of the squared errors, equal to 2.2×10^{15}. As is shown in Fig. 5, the majority of the stress ranges in the HM groups are below the knee point (219 MPa), whereas, for the LM group, the most damaging cycles are above it. The increase in the second slope therefore mainly stems from the increased modified equivalent stress ranges of the HM groups. More experiments with low mean and lower equivalent stress ranges are required to establish the second slope more firmly.

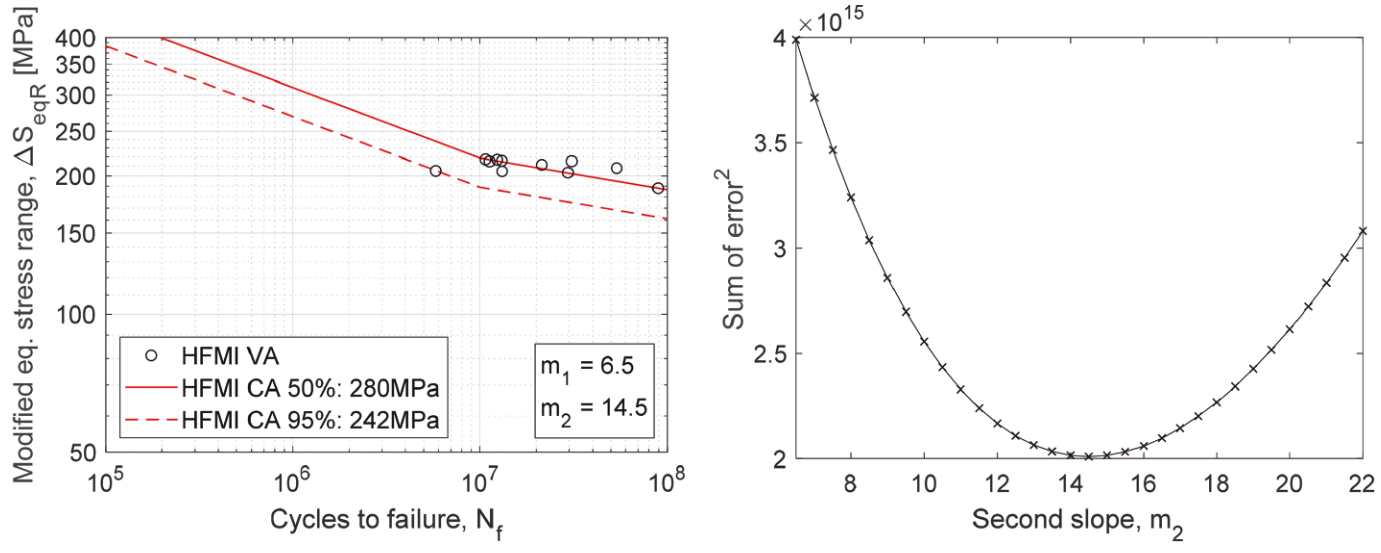

Fig. 14 The second slope that gave the best fit

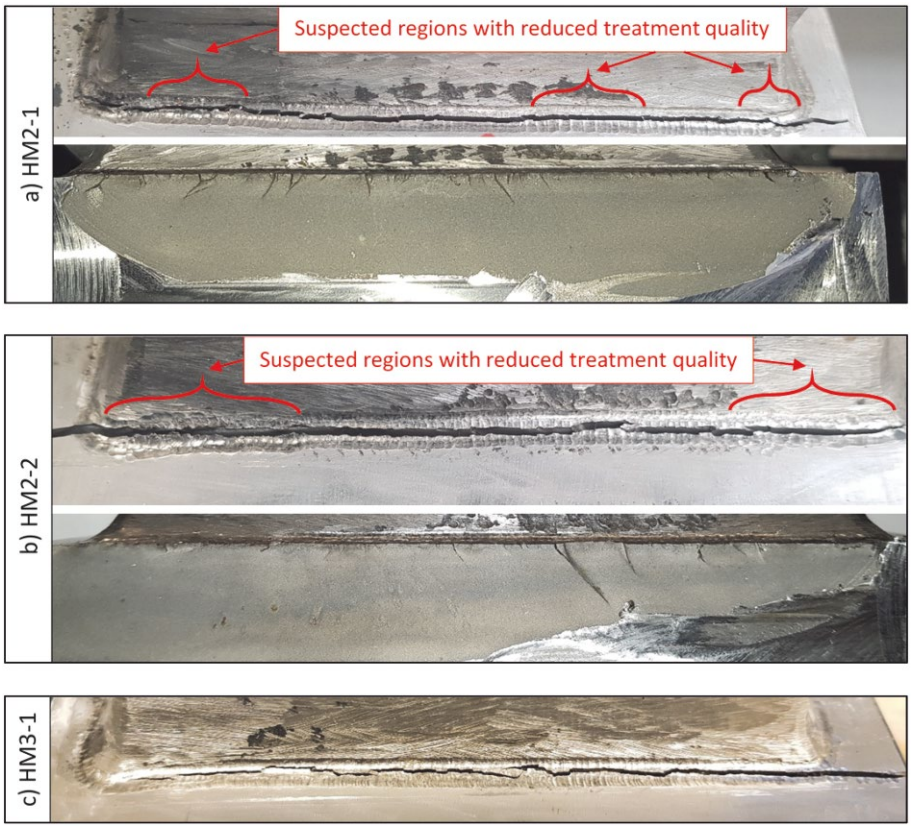

Fig. 15 Final cracks in a) HM2-1 and b) HM2-2 specimens, which failed earlier than expected ($D_{real} = 0.3$ and 0.6 respectively), and c) HM3-1 specimen, which failed later than expected ($D_{real} = 1.9$)

Even after the double-slope evaluation, which produced significantly less scatter in the test results, the HM2-1 specimen, which failed after abnormally few load cycles, remained far from the mean curve, although it was closer to the characteristic curve than before. The HFMI groove and the crack surface of this specimen were therefore closely examined, see Fig. 15a. Prior to opening the crack surface by sawing and milling, there were two hypotheses as to why this specimen failed earlier than predicted by the mean CA HFMI fatigue strength: The first was that the treatment could have been poorly executed and the second was that the cracking mode might have been significantly different, e.g. a sub-surface crack initiation below the weld toe due to an internal defect.

Although it was not possible to establish whether the crack initiated from the surface or sub-surface, the ratchet marks in the fracture surface gave some clues regarding the first hypothesis. Fig. 15a shows that the ratchet marks on the left half of the specimen were all inclined in the same direction, whereas those on the right half were inclined in the opposite direction. This could be an indication that separate dominant cracks initiated on both halves of the weld independently. Looking at the HFMI groove, it can be seen that three regions contained indentation marks that were relatively widely spaced, suspected to be a sign of excessive travel speed during treatment. These regions were also mainly situated on one half of the specimen and could have acted as crack initiation sites [29]. Very similar observations were made for the HM2-2 specimen, which also failed far earlier than expected, i.e. two initiation sites, hinted at by a significant ratchet mark, with a different appearance of the HFMI grooves at these sites, see Fig. 15b. The HFMI grooves of several other specimens related to this study were examined qualitatively in order to make a comparison with the HM2-1 and HM2-2 specimens. In some specimens, individual indentation marks were not visible at all, whereas in others they were only visible in smaller portions of the groove compared with HM2-1 and HM2-2. In some further specimens, individual indentations were clearly visible all along the HFMI grooves, but without the large spacings of HM2-1 and HM2-2, see Fig. 15c for an example. The premature failure of HM2-1 and HM2-2 might therefore have been due to lesser induced compressive residual stresses as a result of a poorer treatment quality locally.

It is expected that variations in treatment quality similar to those suspected here were also included in the data pool on which the IIW fatigue strengths are based [24]. After all, the HM2-1 and HM2-2 specimens achieved fatigue lives that were more than six times longer than those of the AW curve and substantially longer compared with the FAT 140 IIW curve. From this viewpoint, these specimens were probably not that exceptional and probably nor was the quality of their HFMI treatment.

Another hypothesis is that HFMI-treated welds subjected to VA loading might be more sensitive to defects and poor execution compared with welds subjected to CA loading. For instance, if only a small portion along a weld

has lower induced compression due to poor HFMI treatment, a VA overload would result in local yielding at that location and relax the compression. This would in turn result in earlier crack initiation. For a comparable CA load with $R = 0.1$, and a stress range equal to the equivalent one in the VA load, this relaxation would probably not occur, and the same lower quality of treatment locally would therefore not show up in the results. This could be a possible topic for future research.

5.2 The design framework

When it comes to the proposed design framework, the fitted Φ-λ_{HFMI} curves presented in Fig. 12a, which are proposed for design purposes, are limited to the Swedish road traffic conditions investigated. In order to investigate how another traffic condition could affect the Φ-λ_{HFMI} curves, a Weibull distribution was used to produce alternative stress range spectra. Similar to the spectrum presented by Tai and Miki [16] for bridge applications, a scale parameter of 24.4 and shape parameter of 1.54 were used. Three spectra were produced with 10^2, 10^5 and 10^7 randomly generated cycles in each. A stress ratio to stress range relationship for simply supported bridges was assumed, i.e. $R_i = S_{sw}/(S_{sw} + \Delta S_i)$.

Fig. 16a shows that the Φ-λ_{HFMI} curves from the Weibull distribution are dependent on the number of cycles in the spectrum. Fig. 16b gives a hint as to why this is the case. In this graph, the spectrum with 10^2 cycles was omitted, as a meaningful histogram could not be produced for such a small number of cycles. The high number of 10^7 randomly generated cycles resulted in extreme values, which deviated more from the mean value of the spectrum compared with the 10^5 case. As a result, a lower average stress range and thus a lower equivalent stress range was produced in relation to the maximum stress range. The ratios of equivalent stress ranges ΔS_{eq} to maximum ranges ΔS_{max} became 0.46, 0.29 and 0.24 for the 10^2, 10^5 and 10^7 spectra respectively. The reason why the spectra generate higher λ_{HFMI} values is explained schematically in Fig. 16c.

Considering the Φ-λ_{HFMI} curves from the Weibull spectra, the phenomenon related to short influence lines should be recalled from Fig. 10. No such effects, which would otherwise have increased the λ_{HFMI} values, were included in the curves from the Weibull spectra. The conclusion is that, for traffic that generates $\Delta S_{eq}/\Delta S_{max}$ ratios significantly different from those studied here, in combination with short influence lines, the result could be higher λ_{HFMI} values than the proposed design curves. The importance of studying other traffic pools is therefore emphasized.

Further comparisons were made to validate the correctness of the proposed design framework. In Fig. 17, exact values of λ_{HFMI} and Φ for the VA fatigue experiments are plotted against the proposed design curve. Moreover, sections taken from the case-study bridges from the previous publication by the authors [14] are included. The most damage-critical sections were chosen. The bridges were all composite steel and concrete and contained one, five, three and two spans in order of bridge number. All the bridges were continuous except for bridge 1, which was simply supported. The bridge spans related to the extracted sections were 32, 29.1, 13.8 and 28.3 m in order of bridge number. The VA loading in the fatigue experiments was based on the results from bridge 1.

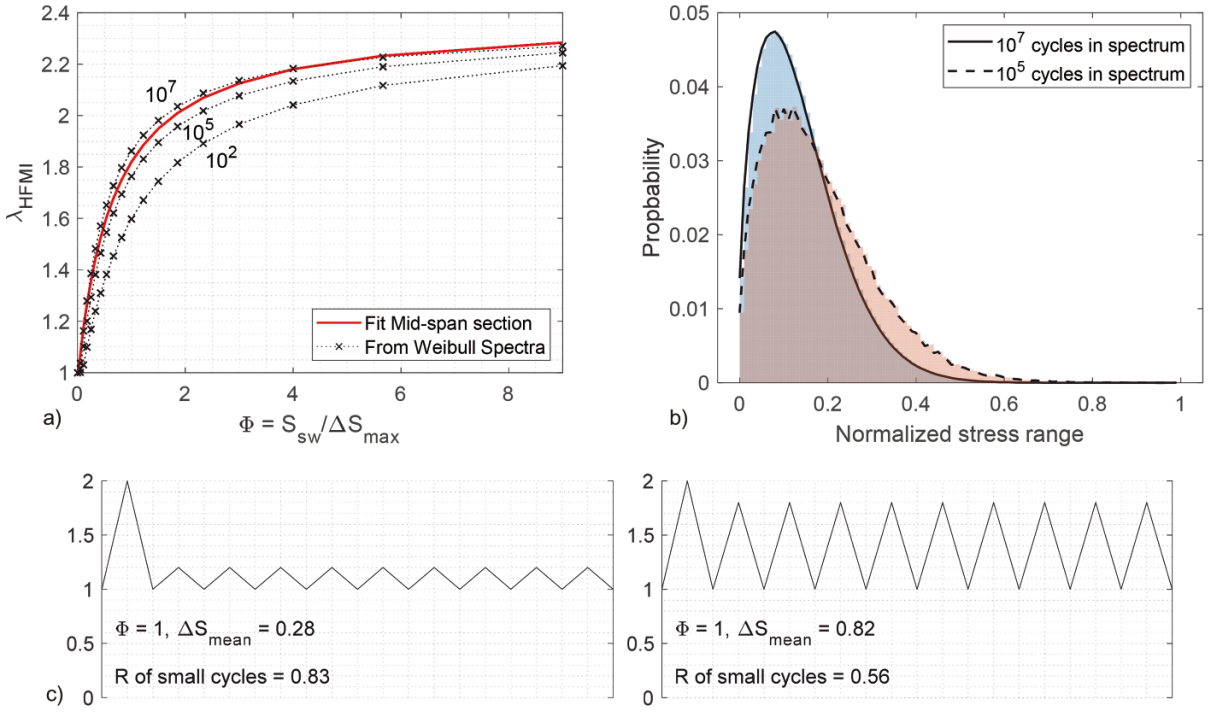

Fig. 16 Comparison of Φ-λ_{HFMI} curves a) from Weibull-distributed stress range spectra, b) with the proposed design curve for mid-span sections, and c) schematic explanation of the effect of the ratio of ΔS_{mean} (or ΔS_{eq}) to ΔS_{max}

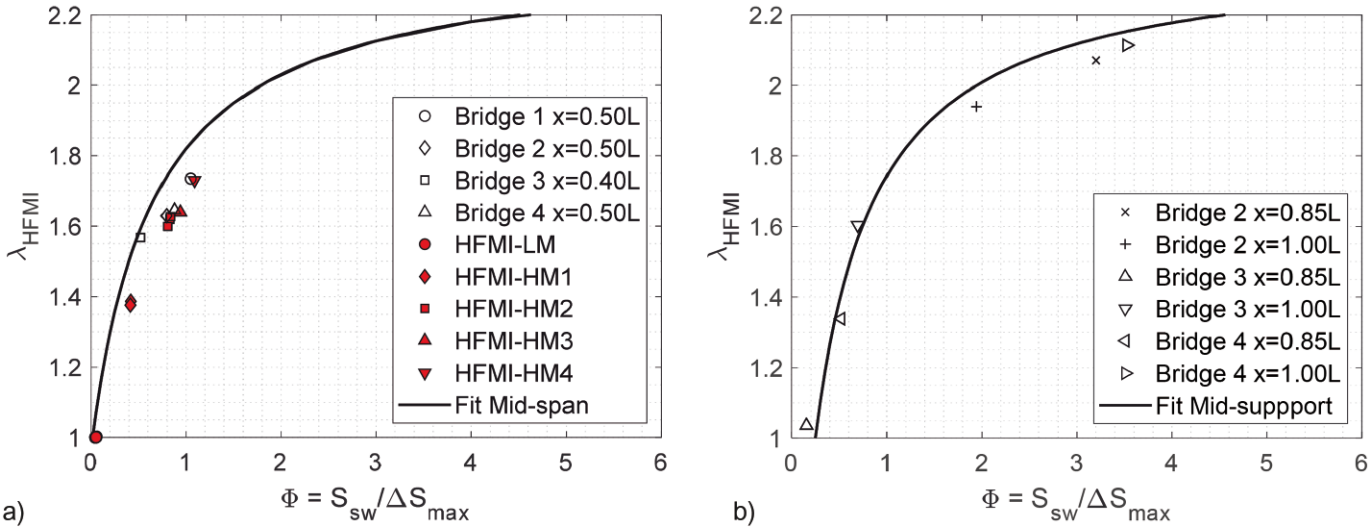

Fig. 17 Exact λ_{HFMI} and Φ-values for the VA experiments and sections from case-study bridges from [14], compared with the proposed design curves: a) mid-span and b) mid-support sections

Firstly, it was found that estimating the Φ values based on $\Delta S_{max} = 2\Delta S_p$, as suggested earlier, did not change the results in Fig. 17 significantly. Tab. 4 provides relevant data and compares the exact and estimated Φ values for the sections from the case-study bridges. The greatest differences were found for the high Φ values of bridge 2 ($x = 0.85L$) and bridge 4 ($x = 1.00L$). Fortunately, this difference had virtually no effect on the resulting λ_{HFMI} values, as the curves flatten out at high Φ values.

Moreover, Fig. 17a shows that, of all the data, bridge 3 was situated closest to the design curve. This was partly because the $\Delta S_{eq}/\Delta S_{max}$ ratio was smallest for bridge 3 (see [14]) and partly because the span was of a size comparable to the $L = 10$ m on which the design curves were based. Fig. 17b shows similar observations for the mid-support sections.

Several parameters were different in the case-study bridges compared with the assumptions behind the design curves. Those assumptions included symmetrical double-span bridges with constant bending stiffness (prismatic beams), whereas bridges 2 and 3 had more spans, including some variations in length of span. More importantly for the continuous bridges, they all had non-constant bending stiffness along the bridge length, which results in significantly different influence lines closer to mid-supports. More information on the bridges can be found in [14]. Taking the comparisons performed in this section, the proposed design framework and the fitted Φ-λ_{HFMI} curves for design appear to be fairly robust and yield reasonable predictions.

The work conducted in this study was based on data obtained from vehicles in Sweden. The data included axle loads, number of axles per vehicle, and the distance between two adjacent axles. However, it will be necessary to investigate traffic data from other countries as well in order to generalize this method and widen its scope. Moreover, the validity of the sample size used for the traf-

Tab. 4 Data of bridge sections (stresses in MPa)

	x/L	S_{sw}	ΔS_{max}	ΔS_p	$\Phi_{exact} = S_{sw}/\Delta S_{max}$	$\Phi_{est} = S_{sw}/(2\Delta S_p)$
Bridge 1	0.50	192	183	94.4	1.05	1.02
Bridge 2	0.50	102	128	66.0	0.80	0.77
Bridge 3	0.40	107	204	93.0	0.52	0.57
Bridge 4	0.50	174	198	102.3	0.88	0.85
Bridge 2	0.85	22	7	3.7	3.20	2.97
Bridge 3	0.85	15	94	49.1	0.16	0.15
Bridge 4	0.85	54	103	55.4	0.52	0.48
Bridge 2	1.00	151	78	38.6	1.94	1.95
Bridge 3	1.00	104	150	71.5	0.69	0.73
Bridge 4	1.00	279	79	34.8	3.52	4.01

fic data investigated (about 55,000 vehicles) needs to be verified. Work is currently being carried out to include more than one million vehicles in the analysis.

6 Conclusions

Experiments studying the variable amplitude (VA) fatigue performance of high-frequency mechanical impact (HFMI)-treated, non-loadbearing transverse attachment specimens was described in this paper, with special emphasis on bridges and the mean stress effect. Backed up by experiments, a design framework for HFMI was presented for the treatment of the mean stress effect under VA loading. The framework included several proposals and suggestions, some applicable in general and some specific to the conditions investigated for bridges. The following conclusions can be drawn:

- The experiments in this paper show that VA loading with low overall mean stresses has no detrimental effect on the fatigue performance of non-loadbearing transverse attachment joints for typical load conditions in road bridges. This includes the combined effects of the specific spectrum shape, the varying mean stresses and the random sequence load. Compared with the constant amplitude (CA) $R = 0.1$ strength of the specimens, an average real damage sum of 1.6 was obtained for low mean stress experiments.
- The experiments clearly and consistently showed the detrimental effect of high overall mean stresses. To include this effect in the load parameter, a proposal was presented for modifying the Palmgren-Miner's equivalent stress range, in combination with a suggested adaptation of the IIW mean stress correction. The modified equivalent stress range could successfully represent the VA load to be compared with the CA $R = 0.1$ strength. Using the modified equivalent stress ranges resulted in an average real damage sum of 1.4.
- Furthermore, it was confirmed experimentally with one test that large compressive preloads dramatically reduce the fatigue life compared with the CA $R = 0.1$ strength. Compressive stresses of high magnitude must therefore be avoided during all stages after HFMI treatment, including transportation, construction and operation.
- The design framework introduces a new factor λ_{HFMI} that has to be multiplied by the Palmgren-Miner's equivalent stress range in order to account for the mean stress effect. The framework allows the designer to obtain λ_{HFMI} without any need for cycle-by-cycle spectrum calculations or prior knowledge of the real VA load. This factor includes the contributions of spectrum shape and the VA load empirically and is dependent on the self-weight stresses. Based on data from Swedish road traffic, expressions for λ_{HFMI} were proposed for the design of bridges.
- The proposed design expressions for λ_{HFMI} were validated by comparison with the experimental results as well as case-study bridges from previous work. The proposed expressions were shown to yield reasonable predictions, even for cases where the conditions were somewhat different.

Nomenclature

AW – as-welded
CA – constant amplitude
FAT – fatigue strength at two million cycles
HFMI – high-frequency mechanical impact
HM – high mean
IIW – International Institute of Welding
LM – low mean
VA – variable amplitude
D – damage factor
f – mean stress correction factor
f_u – ultimate tensile strength
f_y – yield stress
L – span (distance between two bridge supports)
m – slope of *SN* curve
N_f – number of cycles to failure
R – stress ratio
R_{avg} – average stress ratio during testing
R_{max} – maximum stress ratio during testing
R_{min} – minimum stress ratio during testing
S – nominal stress
S_{max} – maximum nominal stress during testing
S_{min} – minimum nominal stress during testing
S_{sw} – self-weight stress
ΔS_{eq} – Palmgren-Minre's equivalent stress range
ΔS_{eqR} – equivalent stress range accounting for stress ratio
ΔS_{max} – maximum nominal stress range during testing or due to traffic
ΔS_{min} – minimum nominal stress range during testing
λ_{HFMI} – ratio of ΔS_{eqR} to ΔS_{eq}
Φ – ratio of self-weight stress to maximum stress range due to traffic

Acknowledgements

This work was partly supported by the Norwegian Public Road Administration in the "Application of Post-weld Treatment for Lightweight Steel Bridges" project, partly by Formas (243-2014-638) and partly by Trafikverket.

References

[1] Skoglund, O. (2019) I*nnovative structural details using high strength steel for steel bridges*. Kungliga Tekniska högskolan, Stockholm.

[2] Yildirim, H. C.; Marquis, G. B. (2012) *Fatigue strength improvement factors for high strength steel welded joints treated by high frequency mechanical impact*. Int. J. Fatigue 44, pp. 168–176. https://doi.org/10.1016/j.ijfatigue.2012.05.002

[3] Shams-Hakimi, P.; Yıldırım, H. C.; Al-Emrani, M. (2017) *The thickness effect of welded details improved by high-frequency mechanical impact treatment*. Int. J. Fatigue 99, Part 1, pp. 111–124. https://doi.org/10.1016/j.ijfatigue.2017.02.023

[4] Shams-Hakimi, P.; Mosiello, A.; Kostakakis, K.; Al-Emrani, M. (2015) *Fatigue life improvement of welded bridge details using high frequency mechanical impact (HFMI) treatment*. The 13th Nordic Steel Construction Conference (NSCC.2015). Tampere University of Technology, Tampere, Finland, 2015, pp. 201–202.

[5] Shimanuki, H.; Okawa, T. (2013) *Effect of stress ratio on the enhancement of fatigue strength in high performance steel welded joints by ultrasonic impact treatment*. Int. J. Steel Struct. 13, No. 1, pp. 155–161. https://doi.org/10.1007/s13296-013-1014-9

[6] Okawa, T.; Shimanuki, H.; Funatsu, Y.; Nose, T.; Sumi, Y. (2013) *Effect of preload and stress ratio on fatigue strength of welded joints improved by ultrasonic impact treatment*. Weld. World 57, No. 2, pp. 235–241.

[7] Mikkola, E.; Doré, M.; Marquis, G.; Khurshid, M. (2015) *Fatigue assessment of high-frequency mechanical impact (HFMI)-treated welded joints subjected to high mean stresses and spectrum loading*. Fatigue Fract. Eng. Mater. Struct. https://doi.org/10.1111/ffe.12296

[8] Deguchi. T. et al. (2012) *Fatigue strength improvement for ship structures by Ultrasonic Peening*. J. Mar. Sci. Technol. 17, No. 3, pp. 360–369. https://doi.org/10.1007/s00773-012-0172-3

[9] Ishikawa, T.; Shimizu, M.; Tomo, H.; Kawano, H.; Yamada, K. (2013) *Effect of compression overload on fatigue strength improved by ICR treatment*. Int. J. Steel Struct. 13, No. 1, pp. 175–181. https://doi.org/10.1007/s13296-013-1016-7

[10] Polezhayeva, H.; Howarth, D.; Kumar, M.; Ahmad, B.; Fitzpatrick, M. E. (2015) *The effect of compressive fatigue loads on fatigue strength of non-load carrying specimens subjected to ultrasonic impact treatment*. Weld. World 59, No. 5, pp. 713–721, 2015. https://doi.org/10.1007/s40194-015-0247-y

[11] Sonsino, C. (2004) *Principles of Variable Amplitude Fatigue Design and Testing*. J. ASTM Int. 1, No. 10. https://doi.org/10.1520/JAI19018

[12] Sonsino, C. M. (2007) *Fatigue testing under variable amplitude loading*. Int. J. Fatigue 29, No. 6, pp. 1080–1089. https://doi.org/10.1016/j.ijfatigue.2006.10.011

[13] Hobbacher, A. F. (2016) *Recommendations for Fatigue Design of Welded Joints and Components (IIW document IIW-2259-15)*. 2nd ed. Switzerland: Springer International Publishing.

[14] Shams-Hakimi, P.; Carlsson, F.; Al-Emrani, M.; Al-Karawi, H. (2021) *Assessment of in-service stresses in steel bridges for high-frequency mechanical impact applications. Engineering Structures* (accepted for publication).

[15] Ghahremani, K.; Walbridge, S. (2011) *Fatigue testing and analysis of peened highway bridge welds under in-service variable amplitude loading conditions*. Int. J. Fatigue 33, No. 3, pp. 300–312. https://doi.org/10.1016/j.ijfatigue.2010.09.004

[16] Tai, M. M.; Miki, P. C. (2012) *Improvement Effects of Fatigue Strength by Burr Grinding and Hammer Peening Under Variable Amplitude Loading*. Weld. World 56, No. 7–8, pp. 109–117. https://doi.org/10.1007/BF03321370

[17] Ghahremani, K.; Walbridge, S.; Topper, T. (2015) *High cycle fatigue behaviour of impact treated welds under variable amplitude loading conditions*. Int. J. Fatigue 81, pp. 128–142. https://doi.org/10.1016/j.ijfatigue.2015.07.022

[18] Eurocode 3 (2006) *Design of steel structures – Part 2: Steel bridges*. European Committee for Standardization.

[19] Mori, T.; Shimanuki, H.; Tanaka, M. M. (2012) *Effect of UIT on fatigue strength of web-gusset welded joints considering service condition of steel structures*. Weld. World 56, No. 9–10, pp. 141–149.

[20] Zhao, X.; Wang, D.; Huo, L. (2011) *Analysis of the S–N curves of welded joints enhanced by ultrasonic peening treatment*. Mater. Des. 32, No. 1, pp. 88–96. https://doi.org/10.1016/j.matdes.2010.06.030

[21] Maddox, S. J.; Doré, M. J.; Smith, S. D. (2011) *A case study of the use of ultrasonic peening for upgrading a welded steel structure*. Weld. World 55, No. 9–10, pp. 56–67,.

[22] Shams-Hakimi, P.; Zamiri, F.; Al-Emrani, M.; Barsoum, Z. (2018) *Experimental study of transverse attachment joints with 40 and 60 mm thick main plates, improved by high-frequency mechanical impact treatment (HFMI)*. Eng. Struct. 155, pp. 251–266, https://doi.org/10.1016/j.engstruct.2017.11.035.

[23] ASTM E1049-85 (2017) *Standard practices for cycle counting in fatigue analysis*. West Conshohocken PA ASTM Int., 2017. https://doi.org/10.1520/E1049-85R17

[24] Marquis, G. B.; Barsoum, Z. (2016) *IIW Recommendations for the HFMI Treatment – For Improving the Fatigue Strength of Welded Joints*. Singapore: Springer Singapore.

[25] Mikkola, E.; Doré, M.; Khurshid, M. (2013) *Fatigue Strength of HFMI Treated Structures Under High R-ratio and Variable Amplitude Loading*. Procedia Eng. 66, pp. 161–170. https://doi.org/10.1016/j.proeng.2013.12.071

[26] Shimanuki, H.; Mori, T.; Tanaka, M. (2013) *Study of a Method for Estimating the Fatigue Strength of Welded Joints Improved by UIT*. IIW Doc. XIII-2495.

[27] Yonezawa, T.; Shimanuki, H.; Mori, T. (2019) *Relaxation behavior of compressive residual stress induced by UIT under cyclic loading*. Q. J. Jpn. Weld. Soc. 37, No. 1, pp. 44–51. https://doi.org/10.2207/qjjws.37.44

[28] Haibach, E. (1970) *Modified linear damage accumulation hypothesis considering the decline of the fatigue limit due to progressive damage*. Lab. Für Betriebsfestigkeit Darmstadt Ger. Techn Mitt TM 50, p. 70.

[29] Al-Karawi, H.; von Bock und Polach, R. U. F.; Al-Emrani, M. (2021) *Crack detection via strain measurements in fatigue testing*. Strain 57, No. e12384.

Authors
Dr. Poja Shams-Hakimi
poja.shams@wsp.com
WSP
Ullevigatan 19
411 40 Göteborg, Sweden

Hassan Al-Karawi (corresponding author)
hassan.alkarawi@chalmers.se
Chalmers University of Technology
Department of Architecture & Civil Engineering
Chalmersplatsen 4
412 96 Göteborg, Sweden

Prof. Mohammad Al-Emrani
mohammad.al-emrani@chalmers.se
Chalmers University of Technology
Department of Architecture & Civil Engineering
Chalmersplatsen 4
412 96 Göteborg, Sweden

How to Cite this Paper

Shams-Hakimi, P.; Al-Karawi, H.; Al-Emrani, M. (2022) *High-cycle variable amplitude fatigue experiments and design framework for bridge welds with high-frequency mechanical impact treatment.* Steel Construction. https://doi.org/10.1002/stco.202200003

This paper has been peer reviewed. Submitted: 29. January 2022; accepted: 14. March 2022.